Critical exponents of ferroelectric transitions in modulated $SrTiO_3$: Consequences of quantum fluctuations and quenched disorder*

Wang Jing-Xue(王景雪), Liu Mei-Feng(刘美风), Yan Zhi-Bo(颜志波), and Liu Jun-Ming(刘俊明)†

Laboratory of Solid State Microstructures, Nanjing University, Nanjing 210093, *China*

(Received 18 February 2013; revised manuscript received 14 March 2013)

The ferroelectric transitions of several $SrTiO_3$-based ferroelectrics are investigated experimentally and theoretically, with special attention to the critical scaling exponents associated with the phase transitions, in order to understand the competition among quantum fluctuations (QFs), quenched disorder, and ferroelectric ordering. Two representative systems with sufficiently strong QFs and quenched disorders in competition with the ferroelectric ordering are investigated. We start from non-stoichiometric $SrTiO_3$ (STO) with the Sr/Ti ratio deviating slightly from one, which is believed to maintain strong QFs. Then, we address Ba/Ca co-doped $Sr_{1-x}(Ca_{0.6389}Ba_{0.3611})_xTiO_3$ (SCBT) with the averaged Sr-site ionic radius identical to the Sr^{2+} ionic radius, which is believed to offer remarkable quenched disorder associated with the Sr-site ionic mismatch. The critical exponents associated with polarization P and dielectric susceptibility ε, respectively, as functions of temperature T close to the critical point T_c, are evaluated. It is revealed that both non-stoichiometric $SrTiO_3$ and SCBT exhibit much bigger critical exponents than the Landau mean-field theory predictions. These critical exponents then decrease gradually with increasing doping level or deviation of Sr/Ti ratio from one. A transverse Ising model applicable to the Sr-site doped STO (e.g., $Sr_{1-x}Ca_xTiO_3$) at low level is used to explain the observed experimental data. It is suggested that the serious deviation of these critical exponents from the Landau theory predictions in these STO-based systems is ascribed to the significant QFs and quenched disorder by partially suppressing the long-range spatial correlation of electric dipoles around the transitions. The present work thus sheds light on our understanding of the critical behaviors of ferroelectric transitions in STO in the presence of quantum fluctuations and quenched disorder, whose effects have been demonstrated to be remarkable.

Keywords: critical exponents, quantum fluctuations, ferroelectric phase transitions

PACS: 77.22.−d, 77.80.B−, 71.55.Jv **DOI:** 10.1088/1674-1056/22/7/077701

1. Introduction

The critical phenomena associated with the second-order phase transitions in condensed matters occupy a central place for understanding their nature and for developing related technological applications. The critical scaling behaviors around the critical point (T_c) of the phase transitions imply a divergence of the spatial correlation length (L_c) of the local order parameters, and this divergence initiates the phase transitions at T_c when temperature T is close to T_c at the high-T side. The divergence is characterized by a set of critical exponents which may fall into various universality classes in the scaling theory framework of phase transitions and critical phenomena.[1] From the 1960s to the 1980s, a tremendous amount of theoretical and experimental studies on these scaling behaviors in various systems and models were performed, including the universal scaling hypothesis and renormalization group theory, with repeated and delicate experimental verifications in well-designed phase transition systems.[2–8]

It is widely believed that the critical scaling theory is applicable to the second-order ferroelectric (FE) transitions in a series of displacement-type ferroelectrics. Upon decreasing T down to T_c, FE polarization (P) emerges, and its dependence on T can be described by the scaling law in the T range very close to T_c. Concomitantly, the variation of dielectric susceptibility $\varepsilon(T)$ at T close to T_c exhibits similar scaling behaviors. These scaling laws can be written as

$$\begin{cases} \Delta\varepsilon^{-1} \sim (T - T_c)^{\gamma_+}, & T > T_c, \\ \Delta\varepsilon^{-1} \sim (T_c - T)^{\gamma_-}, & T < T_c, \end{cases} \tag{1a}$$

$$P \sim (T_c - T)^{\beta}, \quad T < T_c, \tag{1b}$$

where $\gamma_\pm$ and β are the critical exponents which are dimension-dependent but otherwise universal. For second-order phase transitions in ferroic systems, one may simply consult to the Landau phenomenological theory in the mean-field approximations (in short the Landau mean-field theory), due to its simplicity and applicability, rather than the universal scaling hypothesis and renormalization group theory. In this framework, $\gamma_\pm = 1$ and $\beta = 1/2$ are predicted and often cited in literatures.[2,4,6] This Landau mean-field theory has been extraordinarily useful and in fact is still the workhorse for understanding the second-order phase transitions, and not only in ferroic systems. In fact, the case with $\gamma_+ = 1$ is equivalent to the well-known Curie–Weiss law.

In parallel to theoretical progress, experimental measure-

*Project supported by the National Basic Research Program of China (Grant Nos. 2011CB922101 and 2009CB623303), the National Natural Science Foundation of China (Grant Nos. 11234005 and 11074113), and the Priority Academic Development Program of Jiangsu Higher Education Institutions, China.

†Corresponding author. E-mail: liujm@nju.edu.cn

© 2013 Chinese Physical Society and IOP Publishing Ltd

ment of these critical exponents in FE systems has not yet been very popular and most of available data were collected from 1960s to 1980s, although the Curie–Weiss law is extensively used ($\gamma_+ = 1$).[6–10] Beyond that, Kleemann and his collaborators carried out a series of theoretical and experimental studies on the dielectric properties and critical exponents of $SrTiO_3$ (STO) and $Sr_{1-x}Ca_xTiO_3$ (SCT) during 1990s and 2000s,[9,11–20] noting that STO is a typical emergent ferroelectric with the simplest lattice structure and shows quite remarkable quantum fluctuations (QFs) while SCT shows remarkable quenched disorder in competing respectively with FE ordering at low T. While most reported experiments have focused on measurement of critical exponents γ_+ (or γ_-), an accurate evaluation of critical exponent β seems to be technically challenging. The major issue is that polarization P as the order parameter is not easily measured without involving external electric field during the measurement, e.g., using the standard hysteresis loop method. Moreover, electric field induces the FE phase transitions even at $T > T_c$, which is definitely not preferred for better evaluating the critical exponents.[21] Therefore, earlier experiments on the critical phenomena in FE phase transitions concentrated on measuring dielectric susceptibility, while experiments on exponent β are rare.[6,8]

Highlighting the experiments that have been published so far on the second-order FE phase transitions, one sees that the Landau mean-field theory still suffers several problems.[22] The most basic issue is that it just does not properly treat fluctuations of the order parameter, nor does it properly treat the short range ordering slightly above T_c. By taking into account the fluctuations of the order parameter appearing at $T > T_c$ (probably at $T < T_c$ too), exponents $\gamma_+ = 4/3$ and $\beta = 1/3$ are predicted by the modified Laudau theory considering the sixth order of the first non-vanishing derivatives of the thermodynamic potential μ,[23,24] while the short range correlation gives a tail on the specific heat above T_c, which is not available in the Landau mean-field theory. In fact, currently available experimental data give $\gamma_+ > 1$, accounting for the contribution of the order parameter fluctuations and short-range ordering above T_c. This physics becomes particularly significant for relaxor ferroelectrics in which the short-range fluctuations of the order parameter associated with local chemical/domain inhomogeneities have already come into being at the Burn point much higher than T_c.[25,26] Consequently, it was argued that no true critical exponents are available due to the existence of nano-domain freezing and defect dynamics in relaxor ferroelectrics.[27,28] It is well known that the Curie–Weiss law has to be modified by a critical exponent $\gamma_\pm$ much bigger than one.

On the other hand, possible random fluctuations and relaxations against the phase transitions below $T < T_c$ are substantial as well, but much less emphasized so far, and their influences on the critical exponents have not yet been well understood. The dipole–dipole interaction, ubiquitous quenched disorder, defect inhomogeneity, lattice mismatch, stress field pinning, etc., in the testing samples, which can never be negligible in the phase transition regime, influence the critical behaviors. These influences are, however, difficult to be explained in the Landau mean-field theory, due to the fact that a well-defined description of these events is challenging. These events may be the sources of inconsistency between the measured data and theoretical predictions, and therefore the measured critical exponents $\gamma_\pm$ and β would be different from the ones predicted by the Landau theory. In this sense, it is significant to perform profound investigations along these lines.

Comprehensively, the critical phenomena of FE phase transitions in the low-T limit can be of more significance, where the quantum fluctuations (QFs) as an intrinsic ingredient[29] possibly have major impact on the critical behaviors. The quenched disorder is on the other hand an important source inevitably existing in doped systems. Taking STO as an example again, the doped systems such as SCT, $Sr_{1-x}Ba_xTiO_3$ (SBT), etc., where the Sr^{2+} site is partially replaced with smaller Ca^{2+} or larger Ba^{2+}, accommodate site-mismatched disorder in addition to the variation of the site ionic radius.[30,31] Fortunately, unlike the random fluctuations and relaxations mentioned above, the QFs and quenched disorder in these systems are at least reachable experimentally, allowing a tentative and quantitative investigation of this effect associated with the critical phenomena.

Theoretically, the QFs are approached by the quantum zero-point vibration model[5] and the well-known Barrett equation was derived to describe the dielectric response at low T,[32,33] while the transverse Ising model (TIM) Hamiltonian accounts for the competition between the quantum tunneling across the two degenerate ground states, and the FE ordering was proposed.[34,35] This model reproduces quite well the low-T dielectric plateau in STO and related doped STO. Experimentally, the critical exponents $\gamma_\pm$ (> 1) in these materials were measured, demonstrating the substantial role of the QFs in competition with the FE ordering.[11–20] Furthermore, a series of other scenarios in modulating this competition by quenched disorder, non-stoichiometry, pressure, stress, etc., have been developed too,[11–20,36–38] but the competing consequence in terms of the critical behaviors associated with the FE phase transitions has not yet been recognized. It is expected that the existence of QFs and quenched disorder may balance the FE ordering to some extent, and thus the long-range FE order may be broken, partially suppressing the divergence of susceptibility $\varepsilon(T)$ at T_c and the dependence of P on T below T_c. This would result in an enhancement of $\gamma_\pm$ and β with respect to the case of pure FE phase transitions alone.

The above descriptions are tentatively illustrated in Fig. 1(a), where P as a function of T for three cases at $T < T_c$ is

plotted, with critical exponent $\beta < 0.5$, $\beta = 0.5$, and $\beta > 0.5$. For the last case, three more specific cases, $0.5 < \beta < 1$, $\beta = 1$, and $\beta > 1$, are included. The Landau mean-field theory gives $\beta = 0.5$. The cases $\beta > 0.5$ and $\beta < 0.5$ represent the appearance of fluctuations or disorder against the FE ordering below T_c and the order parameter fluctuations at $T > T_c$, respectively. Similar plots can be given for $\gamma_{\pm}$ in the presence of QFs. Figure 1(b) shows the schematic phase diagram of a quantum paraelectric system where the QFs are characterized by the tuning parameter g, and g_c labels the quantum critical point (QCP).[38] The following scaling laws yield:

$$\Delta\varepsilon^{-1} \sim \begin{cases} (T - T_c), & g \to 0, \\ (T - T_c)^2, & g \to g_c, \end{cases} \tag{2}$$

which is consistent with Eq. (1) with $\gamma_+ = 1$ for the case of $g \to 0$ and $T_c \to 0$. However, upon increasing QFs, i.e., with increasing g toward g_c, critical exponent γ_+ evolves from 1 to 2. Quite a number of experimental reports indicating the applicability of Eq. (2) have been published.[9,16–20] Similar expectations may be applied to other cases to be addressed in the present work, such as quenched disorder.

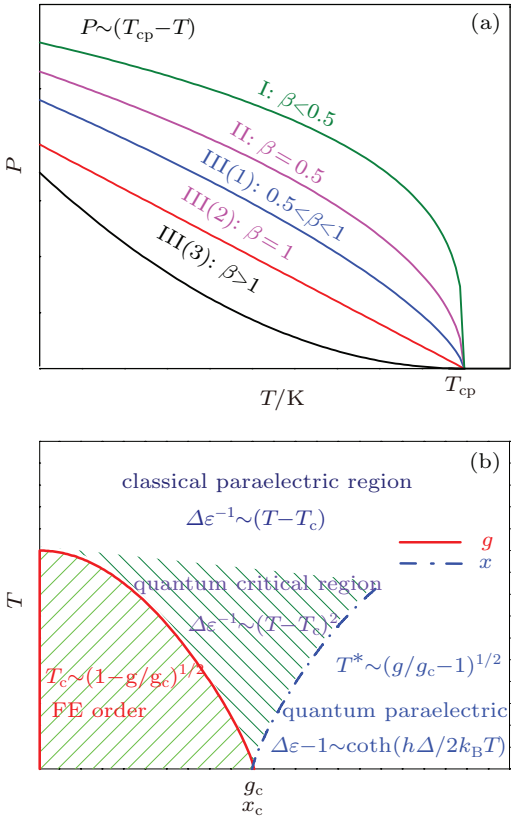


Fig. 1. (color online) (a) A schematic drawing of ferroelectric phase transitions around the critical point T_{cp} with different values of the critical exponent β. (b) Schematic phase diagram of the ferroelectric quantum phase transitions where the QFs are characterized by tuning parameter g (here x is the proposed substitution level at the Sr site in STO) and the critical behaviors of dielectric susceptibility ε are highlighted. The quantum critical point is g_c (x_c) and the scaling relations in various regimes are inserted for reference.

Consequently, in the present work, we are in a good position to address two major issues associated with the critical phenomena of the second-order FE phase transitions in the presence of QFs and quenched disorder. First, we focus on an evaluation of critical exponent β by carefully measuring P as a function of T below T_c using highly sensitive pyroelectric current method developed recently for improper multiferroics at low T.[39,40] This exponent has rarely been measured using this method in literatures. Second, we shall investigate the effects of QFs and quenched disorder on the critical behaviors in various STO-based FE systems in order to see the evolution of the critical scaling behaviors in response to tuning of the QFs and quenched disorder. These data collected in the present work raise questions about the Landau mean-field theory and thus on coupling of the QFs plus quenched disorder into the modern theory of FE phase transitions and critical phenomena.

The remaining part of this article is organized as follows. In Section 2, we describe two experimental objects chosen for the present study and illustrate the reason for such choices, followed by detailed description of the experimental procedures. The main results and discussion will be presented in Section 3. In Section 4, we apply the modified transverse Ising model to calculate the critical behaviors around the critical point in the framework of mean-field approximation, while the effect of quenched disorder still remains open in terms of theoretical description. The theoretical consideration of the QFs and their incorporation into the model for the critical scaling behaviors will be given in Section 5. The summary and conclusion will be given in Section 6.

2. Materials and experimental procedures

Without losing generality, we choose two sets of FE systems for the present experimental investigation, so that the conclusion to be made offers general significance to some extent. These systems can be STO-based and modified by either non-stoichiometry of Sr^{2+} or Ti^{4+}, or Ca^{2+}/Ba^{2+} co-substitution of Sr^{2+}. Relevant experiments and theoretical calculations on the ferroelectric phase transitions themselves have been extensively reported.[31,35–37]

The objects in the first set are non-stoichiometric STO for which the Sr/Ti atomic ratio (x) deviates from one and varies from $x = 0.93$ to 1.06. While STO is believed to exhibit remarkable QFs at low T, this non-stoichiometry results in a slight deviation from the quantum paraelectric state (QPE), accompanied by weak FE ordering, which allows a tuning of the QFs so that an evaluation of the critical scaling behaviors in the presence of strong QFs can be made. The advantage of this system over conventional SCT or SBT is the absence of additional species in non-stoichiometric STO, excluding relevant complexity.[34–37] Since ratio x is limited within a narrow range ($0.93 < x < 1.06$) centered at one, the quenched disorder, if any, is not significant. Therefore, the effect of QFs on

the critical phenomena can be relatively isolated from other processes.

The second set of the FE systems are Ca^{2+}/Ba^{2+} co-substituted STO. Noting that the Sr^{2+} ionic radius is $\langle r_{Sr^{2+}}\rangle = 0.112$ nm, we choose the co-substitution of Ca^{2+} and Ba^{2+} to be smaller and larger than Sr^{2+}, respectively ($\langle r_{Ca^{2+}}\rangle = 0.099$ nm, $\langle r_{Ba^{2+}}\rangle = 0.135$ nm). Our strategy is to keep the average A-site ionic radius identical to that of Sr^{2+}. This leads to a set of samples $Sr_{1-x}(Ca_{0.6389}Ba_{0.3611})_xTiO_3$ (SCBT, $0.002 \leq x \leq 0.10$). Based on this strategy, we can define the Sr-site size-mismatch disorder by parameter $\sigma^2 = \sum_i x_i r_i^2 - \langle r_{Sr^{2+}}\rangle^2$, where x_i and r_i are the atomic fraction and ionic radii of i-type ions at the Sr site, respectively, while all the samples have the identical average Sr-site size $\langle r_{Sr^{2+}}\rangle$. Alternatively, one can simply use doping level x to scale the degree of disorder. Our earlier investigation indicated that such a disorder leads to FE transition behaviors different from those in SCT and SBT.[31] In consequence, local disorder and local lattice distortion appear, as well as weak FE dipole interaction embedded in the STO matrix. By this scenario, the quenched disorder and its competition against the FE ordering can be modulated tentatively.

2.1. Non-stoichiometric $SrTiO_3$

High-quality polycrystalline non-stoichiometric STO samples with different Sr/Ti ratio x (from 0.93 to 1.1) were prepared by the two-step molten salt method.[36,37] First, highly purified $SrCO_3$, TiO_2, and NaCl powder were mixed, ground, and calcined at 880 °C for 7 h in air. Then, the products were washed repeatedly with hot deionized water to remove NaCl. After that, additional NaCl powder was added to the resultant products, and the mixtures were calcined again at 950 °C for 10 h in air. Finally, the fully washed powders were pressed under 20 MPa into disks of 20-mm diameter and 1.5-mm thickness and then sintered at 1150 °C for 20 h in air. All of samples in this series were prepared with an identical procedure, and the measured x values fit well with the nominal compositions within ±0.5% uncertainties of energy dispersive X-ray spectrometry.

The microstructural characterization of this set of samples was reported in our earlier work.[36,37] It was demonstrated that the samples offer high quality and homogeneity, qualified for obtaining highly reliable data in the critical exponent measurement.

2.2. $Sr_{1-x}(Ca_{0.6389}Ba_{0.3611})_xTiO_3$

A series of polycrystalline $Sr_{1-x}(Ca_{0.6389}Ba_{0.3611})_xTiO_3$ (SCBT) samples were prepared by the conventional solid-state reaction method. Reagent grade $SrCO_3$, $CaCO_3$, $BaCO_3$, and TiO_2 were weighed according to the chemical stoichiometric ratio. The as-prepared powders were dried and then calcined at 1150 °C for 10 h. The resultant powders were reground and pelletized under 20 MPa pressure into disks of 2 cm in diameter and then sintered at 1400 °C in air for 6 h. Similarly, the microstructural characterization of this set of samples was reported in our earlier work.[31] The dielectric measurements of these samples were performed by the standard procedure using the HP 4294A impedance analyzer in connection with a Quantum Design physical property measurement system (PPMS).

2.3. Pyroelectric current measurement

In order to exclude the influence of electric field on FE phase transitions as is usually done in the hysteresis loop method, we employ the low-T pyroelectric current method to evaluate the polarization. The thin plate-like samples (with thickness down to 0.2 mm) were coated with top and bottom Au electrodes and the measurement was performed in the cryogenic vacuum chamber of a PPMS. The sample was first cooled down to $T = 2$ K under a poling electric field (about 10 kV/cm) using a Keithley 2400 electro source, followed by a short-circuit procedure of sufficiently long duration until the current (*in-situ* monitored by a Keithley 6514) was below 1.0 pA. Then, the pyroelectric current I (measured by a Keithley 6514) was recorded in the warming sequence at a fixed warming rate. Similar measurements were performed at three different warming rates so that any contribution from sources other than the pyroelectric current can be excluded. Finally, the measured $I(T)$ data were used to obtain $P(T)$ by a simple integration scheme. This method has been demonstrated repeatedly in Refs. [36], [37], [39], and [40].

It should be mentioned that one of the major advantages of the pyroelectric current method is that polarization P can be evaluated without involving an electric field during the probing. However, the drawback is that this method may induce some errors if T_c is high (> 100 K), where current sources other than the pyroelectric effect may no longer be negligible. This is the reason why we choose STO-based materials with a low doping level for the present investigation.

2.4. Evaluation of critical exponents

A reliable procedure to evaluate the critical exponents is the top priority. In fitting to the critical exponents, we take different fitting procedures for the dielectric susceptibility and polarization as a function of T, respectively. For $P(T)$, we take the data within the T range of $(0.7T_{P=0}, T_{P=0})$, where $T_{P=0}$ is the point where $P = 0$, i.e., the critical point T_{cp} defined from the polarization data, and perform the fitting procedure with Eq. (1b). In fact, narrowing or extending the lower limit does not cause much difference in the exponents.

For evaluating exponents $\gamma_\pm$, the fitting is done within the T range of $(0.7T_{c\varepsilon}, 1.3T_{c\varepsilon})$, where $T_{c\varepsilon}$ is the point of the peak of function $\varepsilon(T)$, i.e., the critical point $T_{c\varepsilon}$ defined from the dielectric data.

The ε–T fitting is performed using the method of Ménoret,[10] namely,

$$\frac{1}{\varepsilon}-\frac{1}{\varepsilon_{\rm c}}=\begin{cases}\dfrac{(T_{{\rm c}\varepsilon}-T)^{\gamma_-}}{C^-}, & T\le T_{{\rm c}\varepsilon},\\ \dfrac{(T-T_{{\rm c}\varepsilon})^{\gamma_+}}{C^+}, & T\ge T_{{\rm c}\varepsilon},\end{cases} \tag{3}$$

where $\varepsilon_{\rm c}$ is the value of ε at $T_{{\rm c}\varepsilon}$, and it works very well for the dielectric data in the vicinity of the phase transition, giving the critical exponents $\gamma_+(T\ge T_{{\rm c}\varepsilon})$ and $\gamma_-(T\le T_{{\rm c}\varepsilon})$.

It should be mentioned that the evaluated $T_{{\rm c}\varepsilon}$ from Eq. (3) is usually different from $T_{\rm cp}$. This difference becomes particularly remarkable if the P–T data are measured using the hysteresis method with an external electric field. Fortunately, for normal FE systems, the measured $T_{{\rm c}\varepsilon}$ is only slightly lower than $T_{\rm cp}$, and the difference is within 2 K. The main reason is that the P–T data here are measured using the pyroelectric current method, without involving an external electric field. In this case, the big difference between $T_{{\rm c}\varepsilon}$ and $T_{\rm cp}$, if any, implies the appearance of additional physical factors, such as the disorder-induced fluctuations of the order parameter in SCBT, to be addressed below.

3. Experimental results and discussion

3.1. Non-stoichiometric $SrTiO_3$

Our earlier experiments on high-quality non-stoichiometric STO samples with different Sr/Ti ratios ($0.93\le x\le 1.10$) revealed weak ferroelectricity at low T, indicating the appearance of FE ordering in competition with the QFs with increasing $|1-x|$.[36,37] Given the well-known fact that STO is an incipient ferroelectric (quantum paraelectric) in which ferroelectricity is suppressed by strong QFs, this series of slightly non-stoichiometric STO samples allows us a possibility to evaluate the response of the critical exponents to the QFs, noting again that the quenched disorder in this set of samples is relatively weak.

Figure 2(a) shows the measured P–T data at several x values as labeled in the plot. The corresponding fitting curves using Eq. (1b) near $T_{\rm cp}$ are also presented. It is shown that the measured P is very small, which would be impossible to probe using the hysteresis method in the current state, and the fitting curves reproduce the measured data very well. Prior to analyzing the critical behaviors near $T_{\rm cp}$, we need to mention that the sample with x=1.0 also exhibits small P at low T. This can probably be ascribed to the tiny deviation of the Sr/Ti from one, although the nominal value is one.[36,37] In addition, even stoichiometric STO is in a marginal state, delicately balanced by the incipient ferroelectricity and QFs. The inevitable defects and grain boundaries in the samples may contribute to the inhomogeneity. As a result, it is not surprising to detect a small non-zero polarization of 2×10^{-4} μC/cm^2.

Along these lines, Fig.2(b) plots the evaluated $T_{\rm cp}$ and exponent β against x, noting that the value of $T_{\rm cp}$ at $x=1.0$ is 12.5 K instead of zero in the ideal case, due to the very long tail of the P–T curve and other reasons mentioned above. Anyway, it is found that $T_{\rm cp}$ increases rapidly with increasing $|1-x|$ for both sides. This effect is more significant for $x<1.0$ than that for $x>1.0$, indicating stronger ferroelectricity at $x<1.00$ side. Since Ti^{2+} is smaller than Sr^{2+}, anti-site interstitial Ti^{2+} may prefer a bigger off-center ionic displacement in the tilted-TiO_6 octahedron, thus more easily stabilizing the FE phase against the QFs.[41–43] Regarding the critical exponent β as a function of x, as shown in Fig. 2(b), one observes the gradual decrease of β upon $|1-x|$ from both sides, and the maximal value of 2.79 appears at $x=1.0$, in an opposite way from $T_{\rm cp}(x)$.

As shown in Fig. 2(b), a β value much bigger than 0.5 reveals that the FE phase transition deviates from the second-order type and the QFs are very strong. This exponent decreases gradually with increasing tendency toward FE ordering rather than the QFs as $|1-x|$ increases. It is expected that this tendency would continue, eventually reaching the state of $\beta=0.5$, if the QFs are sufficiently suppressed. Unfortunately, over the whole x range or the biggest off-stoichiometry limit that can maintain a pure single-phase perovskite structure in the present work, the minimal β is 1.94, still much bigger than 0.5. Similar data were reported in $Sr_{1-x}Ca_xTiO_3$ at $x=0.002$ and in ^{18}O isotope-exchanged STO.[9,19]

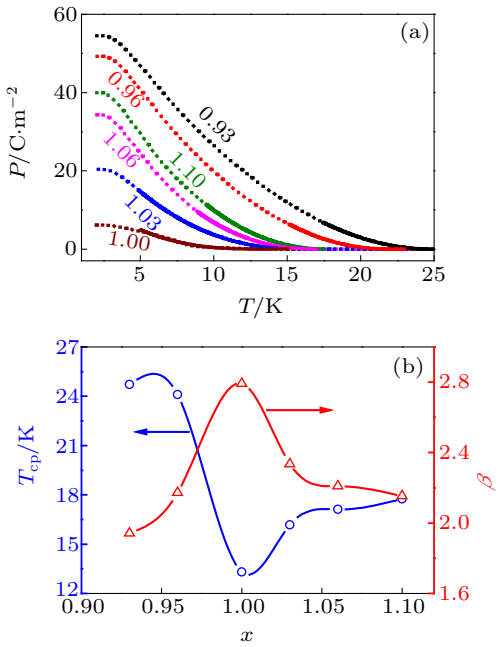


Fig. 2. (color online) (a) Measured P–T data (dots) around the critical points $T_{\rm cp}$ for a series of non-stoichiometric STO samples with the Sr/Ti ratio x labeled numerically. The solid lines are the fitted curves. (b) Evaluated critical point $T_{\rm cp}$ and exponent β as functions of x.

In addition, we evaluate the critical exponents $\gamma_\pm$ by fitting the dielectric susceptibility as a function of T around $T_{{\rm c}\varepsilon}$ using Eq. (3). Figure 3(a) plots the measured data close to $T_{{\rm c}\varepsilon}$ and the fitting curves for a series of samples. The as-evaluated exponents $\gamma_\pm$ as functions of x are presented in Fig. 3(b). As

expected, both $\gamma_{\pm}(x)$ show the dependencies on x similar to that of exponent β. Their values at $x = 1.0$ are much bigger than the Landau theory predicted value 1.0, and they decrease with increasing $|1-x|$ for both sides. This again demonstrates the substantial role of QFs in competition with the ferroelectric ordering in STO, although this role decays gradually along with $|1-x|$, corresponding to the enhanced ferroelectricity.

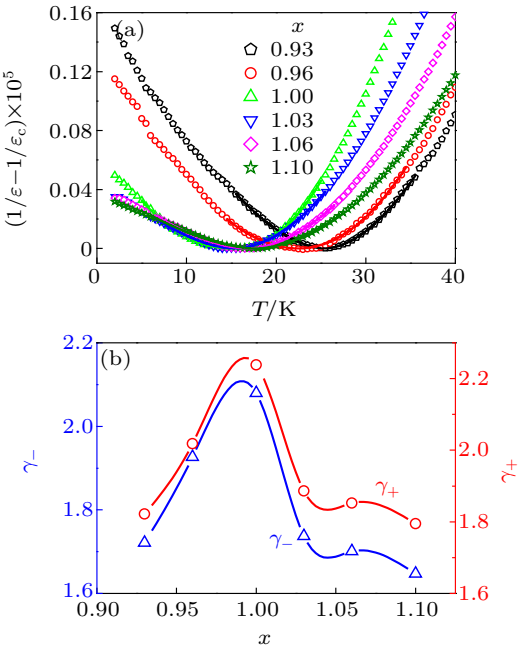


Fig. 3. (color online) (a) Measured $\varepsilon - T$ data (dots) around the critical points for a series of non-stoichiometric STO samples with the Sr/Ti ratio x labeled numerically. The frequency of the AC signals is 1.0 kHz. The solid lines are the fitting curves. (b) Evaluated critical exponents γ_+ and γ_- as functions of x.

The most unusual characteristic of the present systems is the fact that $\beta \geq \gamma > 1.00$. Similar extraordinary behaviors were found in an earlier investigation of SCT, where $\gamma = \beta = 1.65$ at $x = 0.002$, $\gamma = 1.2$ and $\beta = 1.3$ at $x = 0.007$, satisfying the relation $\beta \geq \gamma > 1.00$.[9] It was argued that a novel approach involving dimensionalities higher than those of conventional magnetic, dipolar, or percolative systems is needed. Nevertheless, it was also reported that $\beta = 1.2$ and $\gamma = 1.9 \pm 0.1$ in ^{18}O isotope-exchanged STO (i.e., $SrTi(^{16}O^{18}_{0.06}O_{0.94})_3$),[18] contrary to this relation. A reasonable explanation of these contradictory results is required.

3.2. $Sr_{1-x}(Ca_{0.6389}Ba_{0.3611})_xTiO_3$

We come to the effect of quenched disorder on the critical phenomena in the SCBT sample set, noting that the QFs in these samples are also non-negligible, in particular at low x levels. It was found that the FE transition point $T_{c\varepsilon}$ (or T_{cp}) exceeds ~ 30 K at $x > 0.02$, indicating that the QFs, if any, in these cases are no longer very remarkable. The dominant process is the quenched disorder.

The measured $\varepsilon(T)$ data near $T_{c\varepsilon}$ for several samples with $x \geq 0.02$ are plotted as dots in Fig. 4(a) in the format of $(1/\varepsilon - 1/\varepsilon_c)$ against T, and the corresponding best fitting curves using Eq. (3) are plotted as solid lines, showing the excellent consistency between them. While it is seen that $T_{c\varepsilon}$ shifts remarkably with increasing x, the dielectric peak becomes much sharper too. This indicates that the FE ordering is gradually enhanced, approaching the normal FE state when the doping level is higher than ~ 0.10.

Based on these data, the two exponents $\gamma_{\pm}$ as functions of x are both evaluated and presented in Fig. 4(b). It is observed that both exponents remain roughly constant over the whole range covered in the present experiment, and their values are ~ 2.0, much bigger than the value (1.0) predicted by the Landau mean-field theory. Since the degree of disorder is enhanced with increasing x (scaled by σ^2), while the FE ordering tendency is enhanced too, it seems that the competition between the FE ordering and quenched disorder-induced fluctuations of order parameter takes a balanced state, allowing a dominant role of the disorder in partially suppressing the long-range order established at the critical point.

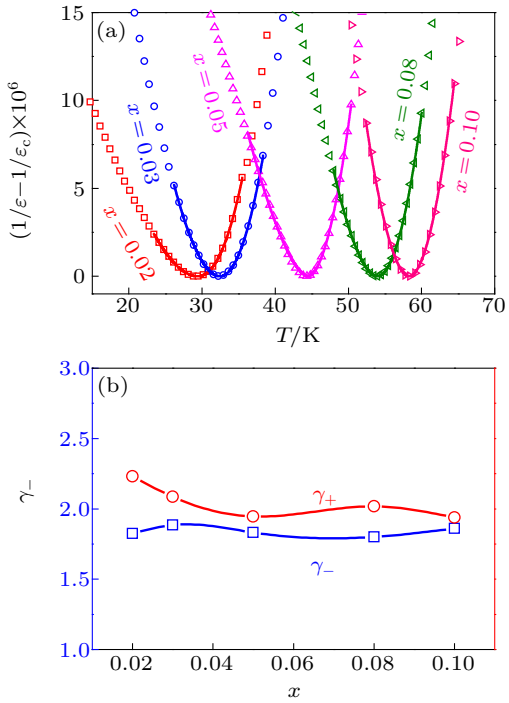


Fig. 4. (color online) (a) Measured $\varepsilon - T$ data (dots) around the critical points for a series of SCBT samples with the co-doping level x labeled numerically. The frequency of the AC signals is 1.0 kHz. The solid lines are the fitted curves. (b) Evaluated critical exponents γ_+ and γ_- as functions of x.

To further reveal this feature, we investigate the P–T behaviors for a series of SCBT samples and the data are plotted in Fig. 5(a). These curves can be very well fitted using the scaling relation (Eq. (2)), and both the evaluated critical point T_{cp} and exponent β as functions of x are presented in Fig. 5(b). It is clearly seen that T_{cp} is much higher than $T_{c\varepsilon}$ and the gap between them is 10–30 K. The evaluated exponent β is from 3.0 to 5.0, much bigger than 0.5 predicted by the Landau

mean-field theory. These facts demonstrate that the quenched disorder significantly influences the critical behaviors.

To understand these behaviors qualitatively, one consults the scenario of phase transitions. For a conventional FE phase transition, an order parameter develops as a collective effect of the entire system, as characterized by a diverging correlation length of the order parameter fluctuations and singularities of the thermodynamic observables at T_c. However, upon a low impurity doping, the QPE state may evolve into spatial regions with impurities centered, which are coupled with the matrix via an overdamped dynamics and undergo phase transitions at different values of the control parameter, such as T here, while the correlation between these regions may not be negligible. As long as the system permits the so-called rare regions with quenched random fields, which are locally in the ordered phase and whose order parameters can be aligned by an infinitesimally small interaction, a true phase transition independent of the bulk would occur. A true static order will develop in these rare regions. Therefore, the global order develops inhomogeneously over a finite T range, i.e., such quenched and locally ordered regions can lead to a smeared global phase transition and a non-zero polarization.[44]

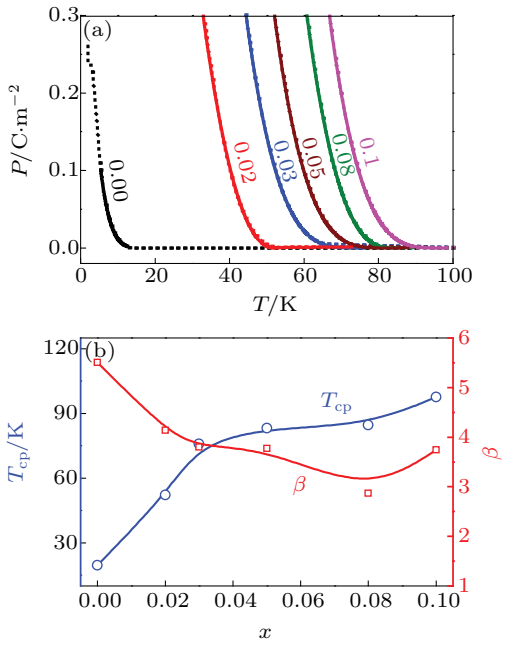


Fig. 5. (color online) (a) Measured P–T data (dots) around the critical points T_{cp} for a series of SCBT samples with the co-doping level x labeled numerically. The solid lines are the fitted curves. (b) Evaluated critical point T_{cp} and exponent β as functions of x.

If the above scenario is applied to SCBT samples here, and the non-zero P will appear at T_{cp} which is above T_c, because of the over-damping of the dynamics due to the coupling of the order parameter with the quenched disorder. Therefore, one observes a remarkable gap between T_{cp} and $T_{c\varepsilon}$. The consequence of this scenario is the unusual critical behavior close to T_{cp} indicated by an exponent β much bigger than 0.5. In fact, similar results in relaxor ferroelectrics and SCT may originate from the same scenario.[9,25,26]

4. Transverse field Ising model and numerical calculations

Our data on the two sets of STO-based systems show clearly the substantial influences of QFs and quenched disorder on the critical phenomena. While the effect of the quenched disorder remains an issue in terms of theoretical description, one is in a position to deal with the effect of QFs by means of the transverse field Ising model (TIM), which has been extensively employed to investigate the physics of QFs in quantum ferroelectrics.[11–14,35–37] In this section, we start from this model and perform a mean-field calculation on the FE phase transitions in SCT or SBT at low doping level, so that the critical exponents can be evaluated as a function of the doping level.

4.1. Model and mean-field calculations

The TIM and its mean-field theory on the competition between the FE ordering and QFs in SCT and SBT were reported by good consistency between the calculations and experiments.[11,12,14,34,45] Here, the calculation is focused on $Sr_{1-x}Ca_xTiO_3$ (SCT), while a similar calculation on $Sr_{1-x}Ba_xTiO_3$ (SBT) can be done too.[35] In description, we assume that the $CaTiO_3$ (CTO) unit cells are distributed randomly in the host STO lattice. It is noted that Ca^{2+} in a CTO cell would take a certain off-center displacement inducing a tilting of the TiO_6 octahedra.

This TIM considers two types of dopant occupancy in SCT: case I is an isolated CTO unit cell surrounded by host STO cells; case II is opposite tilted-TiO_6 octahedra rotation of the two or more neighboring CTO unit cells, inducing antipolar clusters and a local antiferrodistortive (AFD) effect. Considering the competition between FE ordering and the AFD effect plus the role of QFs in SCT, this modified TIM describing the quantum phase transitions of SCT takes the following Hamiltonian:[35]

$$H = -\sum_{<i>}\Omega_{hi}s^x_{hi} - \sum_{<ij>}J^{hh}_{ij}s^z_{hi}s^z_{hj} - \sum_{<i>}\mu^h_i E_i s^z_{hi} - \sum_{<i>}\Omega_{di}s^x_{di} - \sum_{<ij>}J^{hd}_{ij}s^z_{hi}s^z_{dj} - \sum_{<i>}\mu^d_i E_i s^z_{di} - \sum_{<i>}J^{dd}_{ij}s^z_{di}s^z_{dj}, \quad (4)$$

where J^{dd} is the interaction between the dopant pseudospins and $J^{dd} < 0$ is assumed, favoring the anti-polar alignment between two neighboring CTO cells. The configuration $\langle ij \rangle$ in the equation refers to the interactions between one pseudospin and its q neighbors.

Considering an N-pseudospin three-dimensional lattice, the numbers of the dopant pseudospins for the two cases, $n_d(\mathrm{I})$ and $n_d(\mathrm{II})$, are given by $n_d(\mathrm{I}) = Nx(1-x)^q$ and $n_d(\mathrm{II}) = Nx[1-(1-x)^q]$. The number of CTO unit cells is the sum

of $n_d(\mathrm{I})$ and $n_d(\mathrm{II})$ and the number of inter-pseudospin bonds is $f = Nq/2$ which can be sub-divided into four types: i) number of host-host bonds is $f_{hh} = Nq(1-x)^2/2$, ii) number of host-dopant bonds in case I is $f_{hd}(\mathrm{I}) = Nqx(1-x)^q$, iii) number of host-dopant bonds in case II is $f_{hd}(\mathrm{II}) = Nqx[1-(1-x)^q] - Nqx^2$, and iv) number of dopant-dopant bonds in case II is $f_{dd} = Nqx^2/2$. In total, we have $f = f_{hh} + f_{hd}(\mathrm{I}) + f_{hd}(\mathrm{II}) + f_{dd}$. Then, four-order parameters $\langle s_h \rangle$, $\langle s_I \rangle$, $\langle s_{IIA} \rangle$, and $\langle s_{IIB} \rangle$ can be defined to count the numbers of the four types of pseudospins in this scenario. The effective field for each of the four order parameters F_h, F_I, F_{IIA}, and F_{IIB} can be obtained. On this basis, the self-consistent equation set for the four-order parameters is obtained in the form $\langle S_\mu \rangle = (F_\mu/2|F_\mu|)\tanh(|F_\mu|/2k_BT)$, $\mu = h$, I, IIA, IIB, where k_B is the Boltzmann constant.

Finally, polarization P and dielectric susceptibility ε can be expressed as

$$P = 2\mu^h n_h \langle s_h \rangle + 2\mu^d n_d(\mathrm{I})\langle s_I \rangle + \mu^d n_d(\mathrm{II})(\langle s_{IIA} \rangle + \langle s_{IIB} \rangle), \quad (5a)$$

$$\varepsilon = \frac{1}{\varepsilon_0}\frac{\mathrm{d}P}{\mathrm{d}E} \approx \frac{1}{\varepsilon_0}\frac{\Delta P}{\Delta E} = \frac{1}{\varepsilon_0}\frac{P(E=E_0) - P(E=0)}{E_0}. \quad (5b)$$

We calculate the mean-field polarization P and static dielectric susceptibility ε as a function of T for a series of x, focusing on the data around the critical point, so that the critical exponents can be evaluated with sufficient accuracy.

4.2. Results and discussion

While the full-scale phase diagram of $Sr_{1-x}Ca_xTiO_3$ over x up to 0.40 was given in our earlier work,[35] we show here the calculated data for a very low x range so that the influence of the QFs in competition with the FE ordering can be representatively illustrated. It is noted that similar results are obtained for $Sr_{1-x}Ba_xTiO_3$ at very low x range.

The as-evaluated data are presented in Figs. 6(a) and 6(b), where the dots are calculated data and the solid lines are the fitting results, noting that the lowest nonzero x value for the calculation is 0.002. For $x = 0$, the very small P value at $T \to 0$ is not true for real STO and may come from TIM itself. These calculated $P(T)$ data slightly below T_{cp} at various x are fitted using Eq. 1(b) to obtain parameters β and T_{cp}, as given in Fig. 6(c) as functions of x. Taking the phase diagram (Fig. 1(b)) as a reference and noting that tuning factor g should decrease with increasing x, one easily observes from the evaluated T_{cp}–x curve that the region at extremely low $x \leq 0.003$ accommodates the typical QPE state where T_{cp} (here it is the boundary T^* between the QPE region and quantum critical region as shown in Fig. 1(b)) decreases rapidly with increasing x. In this region, the QFs are very strong, leading to high T_{cp} and much bigger exponent β than that predicted by Landau mean-field theory, i.e., 1/2.

Upon passing across $x = 0.003$ and up to $x \sim 0.01$, the system enters the quantum critical region (QC state), where the evaluated T_{cp} reaches its minimum and the exponent β falls to $\sim 1/2$, consistent with the Landau mean-field theory prediction. This implies that the QFs are seriously suppressed by the FE ordering, and thus the system transforms into the normal FE state as x increases further, exceeding 0.01. In this normal FE region, the typical feature of FE transitions is revealed by the fact that T_{cp} keeps increasing with increasing x (see Fig. 6(b)). Consequently, exponent β is well described by the Landau mean field theory, i.e., $\beta = 0.5$, as shown in Fig. 6(c).

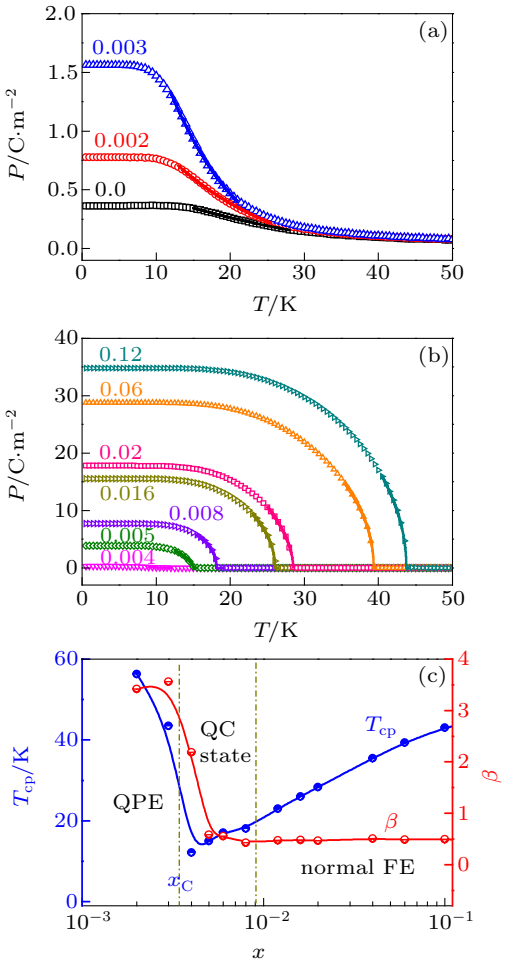


Fig. 6. (color online) (a), (b) Calculated P–T data (dots) around the critical points T_{cp} for a series of SCT samples with the Ca substitution level x labeled numerically. The solid lines are the fitted curves. (c) Evaluated critical point T_{cp} and exponent β as functions of x. Here, the QPE denotes the quantum paraelectrics state, and the QC denotes is the quantum critical state.

Here, it should be mentioned that the evaluated T_{cp} separating the QPE region and the QC state may be too high to be reasonable. For $x = 0.002$, the fitted T_{cp} is as high as 50 K. This difficulty may be ascribed to the fact that the critical fluctuations of the local order parameter do appear at much higher T than the widely believed value of ~ 10 K at which STO begins to enter the QPE state with decreasing T. On the other hand, TIM itself and its mean-field approximations may also contribute to the over-high T_{cp} as evaluated in due course. There-

fore, the T_{cp} boundary between the QPE state and QC state remains questionable in any quantitative sense.

We look at the dielectric permittivity $\varepsilon(T)$ as calculated from Eq. (5b), as shown in Figs. 7(a) and 7(b). The evaluated critical exponents $\gamma_{\pm}$ as functions of x are presented in Fig. 7(c). One can see that γ_+ shows a variation trend similar to that of exponent β, i.e., an upward tendency in the QPE region and a dramatic drop from $x = 0.003$ ($\gamma_+ = 4.254$) to $x = 0.005$ ($\gamma_+ = 1.32$), corresponding to a transition across the boundary between the QPE state and the QC state. As x increases up to 0.005–0.016, one observes $\gamma_+ \sim 1.0$, which then keeps almost constant over the higher doping levels in the normal FE state. Reasonably, it is tough to evaluate the exponent γ_- at extremely low x by fitting since the QPE state and even the QC state may not follow the power law near the critical point (T_c and T^* in Fig. 1(b)). On the other hand, it is reasonable to observe almost constant $\gamma_- \sim 1.0$ in the normal FE region where the Landau mean field theory predicts $\gamma = 1.0$.

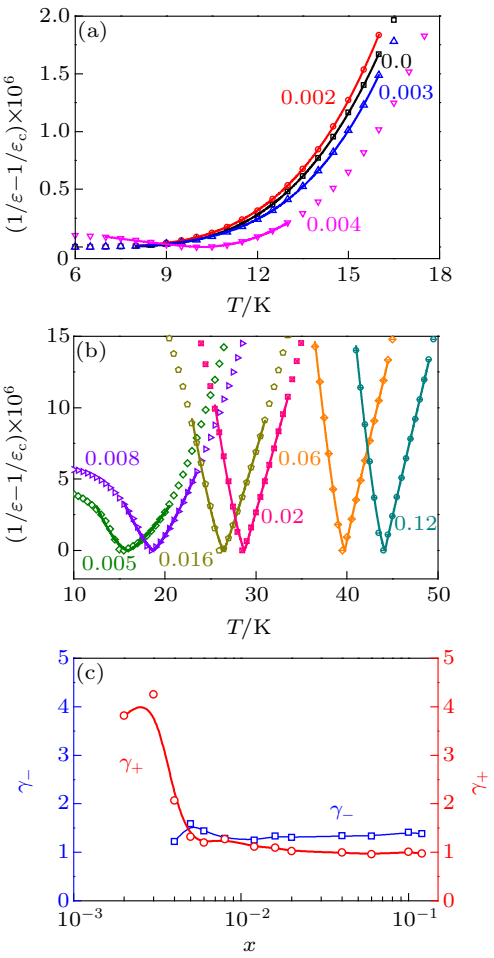


Fig. 7. (color online) (a), (b) Calculated ε-T data (dots) around the critical points for a series of SCT samples with the Ca substitution level x labeled numerically. The solid lines are the fitted curves. (c) Evaluated critical exponents γ_+ and γ_- as functions of x.

Even though the mean-field calculations given here would somehow reduce the range of the local order parameter fluctuations, the TIM model seems to reproduce well the measured exponents quantitatively. The much bigger exponents in the QFs-dominant region are demonstrated experimentally and confirmed here by the calculations based on the TIM. Nevertheless, a microscopically descriptive theory of the underlying physics in terms of the critical phenomena is desirable. We present a preliminary discussion of this issue in the next section.

5. Remarks and quantum-classical mapping

We again start from the schematic phase diagram in Fig. 1(b) for the following discussion. It is obvious that the FE phase transitions in the STO-based systems here belong to the shaded region near $g = g_c$ with $T_c > 0$ K and more importantly with $T_c \to 0$ K. This is quite different from the conventional phase transitions in typical ferroelectrics where T_c can be as high as several hundreds of Kelvin. The finite T region in the vicinity of a quantum critical point therefore offers a fascinating interplay of effects driven by QFs and thermal fluctuations together, leading to nontrivial crossover phenomena absent in conventional FE phase transitions. These crossover behaviors include critical exponents $\gamma \geq 2$ and $\beta \geq 2$ for the non-stoichiometric STO, and $\beta \geq 2$ for slightly doped SCBT, which are different from classical and quantum phase transitions. Here, we discuss how the QFs exert their influence on the critical exponents in the vicinity of the phase transition for the STO-based systems with $T_c \geq 0$ K. It is believed that the quenched disorder in such as SCT, SBT, and SCBT may exert crossover behaviors similar to those in QFs-dominant systems.

In the scaling hypothesis of second-order phase transitions, the critical exponents display the universality property, i.e., they are the same for entire classes of phase transitions which may occur in very different physical systems. These classes, the so-called universality classes, are determined only by the dimension d depending on the range of interactions.[1] In classical systems, the dynamics and the statics are usually decoupled, and thus the dynamic critical exponent is completely independent of the thermodynamic ones. Therefore, the spatial dimension d is equal to the effective dimension d_{eff}. However, for quantum phase transitions, it is known that the Hamiltonian H and its parts H_{kin} and H_{pot} serve as the operators, where H_{kin} is the kinetic energy term and H_{pot} is the potential energy term. The two parts in general do not commute. Consequently, the partition function $Z = Tr\exp(-H/T)$ does not factorize and one must solve the dynamics together with the thermodynamics, which is thus extremely challenging.[46] These quantum systems are space- and time-dependent, and the imaginary time variable τ effectively acts as an additional coordinate and the quantum phase transition is described by an effective theory in a space of higher dimension d_{eff}.[47–49] Therefore, the quantum phase transitions would be in a different universality class from the classic phase transitions, so the critical exponents are in different universality classes too.

It is known that QFs can be coherent over an arbitrarily long scale. For this reason, the effective dimension for the order parameter fluctuations is given by $d_{\rm eff} = d + z$, where d is the spatial dimension and z is the dynamic exponent which characterizes the scaling of energies of the QFs. In the present case, only the choice $z = 1$ leaves the velocity of light c invariant.[47–49] The contribution of the QFs therefore has a profound impact on the critical exponents of the thermodynamic phase transitions.

Since the phase transitions in classical models are driven only by thermal fluctuations, classical systems usually freeze into a fluctuationless ground state at $T \to 0$ K. In contrast, quantum systems have fluctuations driven by the Heisenberg uncertainty principles even in the ground state. Nevertheless, for a finite $T > 0$ and in the vicinity of a quantum phase transition, the interplay between the classical and quantum fluctuations leads to nontrivial crossover phenomena. Using the equivalence between imaginary time and an additional dimension, the homogeneity law for free energy can be in principle generalized to the quantum case, and the scaling behavior of a quantum phase transition in d dimensions can be mapped onto that of some classical transitions in a $(d + 1)$ spatial dimension.[47–50] For the second-order quantum phase transitions, we can let Δ represent a scale characterizing some significant spectral density of fluctuations at $T = 0$ K for $g \neq g_{\rm c}$ (or say Δ is the energy of the lowest excitation above the ground state if it is nonzero). In most cases, as g approaches $g_{\rm c}$, Δ vanishes as $\Delta \sim J|g - g_{\rm c}|^{z\nu}$, where J is the energy scale of a characteristic microscopic coupling, and $z\nu$ is a critical exponent.[46] In addition to a vanishing energy scale, the second-order quantum phase transitions invariably have a diverging characteristic length ξ. This length thus diverges as $\xi^{-1} \sim \kappa|g - g_{\rm c}|^{\nu}$, where ν is the critical exponent and κ is the inverse length scale of the inverse lattice spacing. The characteristic energy scale vanishes as the z-th power of the characteristic inverse length scale $\Delta \sim \xi^{-z}$ $(z = 1)$, i.e., Δ is inversely proportional to the interaction length. This means that the higher the QFs, the smaller the ξ, and by extension, the more rounded the phase transitions and the more notable the difference between the critical exponents and the Landau mean-field theory prediction.

Based on the above discussion and just as manifested in the present experiments, one understands that the QFs play a decisive role. The dynamics and the statics are intricately coupled and the imaginary time direction becomes important for the critical fluctuations, and then the fluctuations of the order parameter makes sense in an effective four dimensional space: $d_{\rm eff} = d + z = 3 + 1 = 4$. This mapping does not represent an exact equivalence in general, but it does become quantitatively precise in the vicinity of the second-order quantum phase transition, i.e., the time axis is the $(d+1)$-th dimension of the corresponding classical model. It is noted that the quantum critical scaling law holds everywhere in the vicinity of the quantum critical point, including at or close to any finite-T phase transition lines that may be approaching the quantum critical point. Although strictly speaking, quantum phase transitions occur only at $T = 0$ K, all realistic experiments are necessarily at $T > 0$ K even very low and close to 0 K. Therefore, for non-stoichiometric STO without strong defects, we can naively argue, according to the quantum critical theory, the critical exponent α, which describes the divergence of the specific heat at constant field, is equal to $-d_{\rm eff} = -4$.[3] Given the fact that $\gamma \geq 2$ was found experimentally earlier[34] and confirmed in the present work, as well as predicted by the quantum spherical model and quantum criticality theory,[38,50,51] plus the TIM calculation here, one has naturally $\beta \geq 2$ from the scaling relation $\alpha + 2\beta + \gamma \geq 2$ (i.e., the Rushbrooke identity). Our experiments sufficiently confirm this prediction.

We report a set of experiments on several STO-based systems which offer significant QFs and quenched disorder. For these systems, the Rushbrooke equality $\alpha + 2\beta + \gamma = 2$ may not work out. The result of $\beta \geq 2$ and $\gamma \geq 2$ does appear for the extreme quantum region $x \leq 0.003$ in $SrTiO_3$: Ca and Sr_xTiO_3 (where x slightly deviates from stoichiometric ratio 1). In this special doping ratio range or for such slight deviation of x from 1, the system gradually changes phase from quantum PE state to quantum FE state and QFs are very strong, i.e., either FE ordering is not dominant or only some scattered polar clusters exist. Such high values of β and γ makes the Rushbrooke equality $\alpha + 2\beta + \gamma = 2$ unlikely.

Although the Rushbrooke scaling relation $\alpha + 2\beta + \gamma \geq 2$ actually holds as an equality in some experiments and in exactly solved models, these experiments and models may not fully take the QFs into account in a comprehensive way. So far, in such high QFs cases, we have no reason or evidence that the Rushbrooke equality holds. Moreover, we observe that $\gamma_- \neq \gamma_+$ for the two systems investigated in our work and this $\gamma_- \neq \gamma_+$ inequality is believed to be reasonable considering the strong QFs or quenched disorder below $T_{\rm c}$, noting that the strength of QFs is intimately related to temperature and that the QFs have a remarkable effect on dielectric susceptibility.

On the other hand, the equality $\gamma_- = \gamma_+$ is a prerequisite for the Rushbrooke equality. Thus, in our opinion, it is still an issue to claim the Rushbrooke equality in a general sense, especially for the cases where the QFs play noteworthy roles.

It comes to our attention that Prof. Kleemann reached the conclusion that $1 < \gamma \leq \beta < 2$ in an earlier report by the scaling relation $\beta = \Delta - \gamma$, based on the curve-fitting parameters γ and Δ over a wide T range on the high temperature side of the dielectric peak, where Δ describes the dependence of dielectric susceptibility $\varepsilon(E)$ upon applied field E.[11,12] Since β only exists below $T_{\rm c}$, one has reason to argue that the equality $\alpha + 2\beta + \gamma_- = 2$ should be an issue too.

Furthermore, it is noted that the T-range chosen for fitting parameters γ and Δ for $SrTiO_3$: Ca in the extreme quantum region is far above the T_c,[11,12] similar to the case that Muller considered for $SrTiO_3$,[53] where the fitting of parameter β was questioned in the literature by Scott.[54] Reliable fitting of the critical exponents should be performed on data in the very vicinity of the critical point.[6–8] In this sense, we claim that the Rushbrooke equality may be an issue for additional investigation, in particular for the cases with remarkable QFs and other quenched disorder sources.

6. Conclusions

In conclusion, we have performed extensive and careful investigations of the critical phenomena associated with the ferroelectric phase transitions in slightly non-stoichiometric STO and Ba/Ca co-doped STO. The former displays the competing QFs and FE ordering and the latter has dominant quenched disorder in competition with the FE ordering. In particular, the critical exponent β describing the scaling behavior of polarization around the critical point has been evaluated by the pyroelectric current technique at low temperature. Much bigger critical exponents than those predicted by the Landau mean field theory have been observed in both non-stoichiometric STO and Ba/Ca co-doped STO, demonstrating the substantial role of either the strong QFs or the remarkable quenched disorder in the critical exponents' positive deviation from the mean-field theory predicted values. We have also performed the TIM calculations which confirm the measured results. A qualitative discussion based on the quantum-classical mapping approach suggests that the crossover between the classical FE phase transitions and the quantum phase transitions is accompanied with the enhanced effective dimension for describing the order parameter fluctuations, leading to much bigger critical exponents in these materials. The present work represents a comprehensive approach to the critical phenomena in second-order FE phase transitions against the background of strong QFs and quenched disorder.

References

[1] Bruce A D and Cowley R A 1981 *Structural Phase Transitions* (London: Taylor and Francis)
[2] Cowley R A 1980 *Adv. Phys.* **29** 1
[3] Schneider T, Beck H and Stoll E 1976 *Phys. Rev. B* **13** 1123
[4] Gonzalo J A 1968 *Phys. Rev. Lett.* **21** 749
[5] Stamenković S, Plakida N M, Aksienov V L and Siklós T 1977 *Acta Physica Academiae Scientiarum Hungaricae Tomus.* **43** 99
[6] Gonzalo J A 1966 *Phys. Rev.* **144** 662
[7] Reese W and May L F 1967 *Phys. Rev.* **162** 510
[8] Schell U and Müser H E 1987 *Z. Phys. B: Condens. Matter.* **66** 237
[9] Dec J and Kleemann W 1998 *Solid State Commun.* **106** 695
[10] Ménoret C, Kiat J M, Dkhil B, Dunlop M, Dammak H and Hernandez O 2002 *Phys. Rev. B* **65** 224104
[11] Wang Y G, Kleemann W, Zhong W L and Zhang L 1998 *Phys. Rev. B* **57** 13343
[12] Kleemann W, Dec J and Westwański B 1998 *Phys. Rev. B* **58** 8985
[13] Wang Y G, Kleemann W, Dec J and Zhong W L 1998 *Europhys. Lett.* **42** 173
[14] Zhang L, Kleemann W and Zhong W L 2002 *Phys. Rev. B* **66** 104105
[15] Prosandeev S A, Maslennikov A E, Kleemann W and Dec J 2000 *Ferroelectrics* **238** 171
[16] Venturini E L, Samara G A and Kleemann W 2003 *Phys. Rev. B* **67** 214102
[17] Kleemann W, Dec J, Wang W and Itoh M 2003 *Phys. Rev. B* **67** 092107
[18] Dec J, Kleemann W and Itoh M 2005 *Phys. Rev. B* **71** 144113
[19] Dec J, Kleemann W and Itoh M 2006 *Ferroelectrics* **337** 13
[20] Venturini E L, Samara G A, Itoh M and Kleemann W 2003 *Fundamental Physics of Ferroelectrics 2003 AIP Conf. Proc.* **677** 1
[21] Fleury P A and Worlock J M 1968 *Phys. Rev.* **174** 613
[22] Martin T D 1997 *American Mineralogist* **82** 213
[23] Kanyuka A K and Glukhov V S 1996 *Physica A* **232** 417
[24] Kanyuka A K and Glukhov V S 1997 *Physica A* **237** 331
[25] Chen W and Cao W Q 2012 *Acta Phys. Sin.* **61** 097701 (in Chinese)
[26] Ahart M, Hushur A, Bing Y, Ye Z G, Hemley R J and Kojima S 2009 *Appl. Phys. Lett.* **94** 142906
[27] Scott J F 2006 *J. Phys.: Condens. Matter* **18** 7123
[28] Kleemann W 2006 *J. Phys.: Condens. Matter* **18** L523
[29] Luo Z H, Cao X J and Yu C F 2011 *Chin. Phys. B* **20** 067103
[30] Wei T, Liu J M, Zhou Q J and Song Q G 2011 *Phys. Rev. B* **83** 052101
[31] Wei T, Zhu C, Wang K F, Cai H L, Zhu J S and Liu J M 2008 *J. Appl. Phys.* **103** 124104
[32] Müller K A and Burkard H 1979 *Phys. Rev. B* **19** 3593
[33] Barrett J H 1952 *Phys. Rev.* **86** 118
[34] Guo Y J, Wei T, Zhu C, Wang K F, Gao X S, Guan Y Q and Liu J M 2010 *J. Appl. Phys.* **107** 074106
[35] Guo Y J, Guo Y Y, Lin L, Gao Y J, Jin B B, Kang L and Liu J M 2012 *Phys. Rev. B* **86** 014202
[36] Guo Y Y, Liu H M, Yu D P and Liu J M 2012 *Phys. Rev. B* **85** 104108
[37] Peng Y P, Wang F X, Zhang L, Peng Y P, Wang C L and Wang Q 1999 *Chin. Phys. Lett.* **16** 214
[38] Rowley S E, Spalek L J, Smith R P, Dean M P M, Lonzarich G G, Scott J F and Saxena S S 2009 *Quantum Criticality in Ferroelectrics* arXiv:0903.1445 [cond-mat.str-el]
[39] Luo S J, Wang K F, Li S Z, Dong X W, Yan Z B, Cai H L and Liu J M 2009 *Appl. Phys. Lett.* **94** 172504
[40] Zhang N, Wang K F, Luo S J, Wei T, Dong X W, Li S Z, Wan J G and Liu J M 2010 *Appl. Phys. Lett.* **96** 252902
[41] Yacoby Y and Just S 1974 *Solid State Commun.* **15** 715
[42] Yacoby Y and Stern E A 1992 *Ferroelectrics* **99** 263
[43] Bednorz J G and Müller K A 1984 *Phys. Rev. Lett.* **52** 2289
[44] Vojta T and Sknepnek R 2004 *Phys. Stat. Sol. (b)* **241** 2118
[45] Wei T, Guo Y J, Wang P W, Yu D P, Wang K F, Lu C L and Liu J M 2008 *Appl. Phys. Lett.* **92** 172912
[46] Sachdev S 2011 *Quantum Phase Transitions* (New York: Cambridge University Press)
[47] Shopova D V and Uzunov D I 2003 *Phys. Rep.* **379** 1
[48] Sperstad I B, Stiansen E B and Sudbø A 2012 *Phys. Rev. B* **85** 214302
[49] Continentino M A 2011 *Braz. J. Phys.* **41** 201
[50] Morf R, Schneider T and Stoll E 1977 *Phys. Rev. B* **16** 462
[51] Stanley H E 1971 *Introduction to Phase Transitions and Critical Phenomena* (Oxford: Clarendon)
[52] Yuan M, Wang C L, Wang Y X, Ali R and Zhang J L 2003 *Solid State Commun.* **127** 419
[53] Müller K A and Berlinger W 1971 *Phys. Rev. Lett.* **26** 13
[54] Scott J F 2007 *Ferroelectrics* **349** 157